Int. J. Heat Mass Transfer. Vol. 33, No. 8, pp. 1685–1695, 1990
Printed in Great Britain

0017–9310/90 $3.00 + 0.00
Pergamon Press plc

Effects of boundary properties on transient temperature distributions in condensed semi-transparent media

D. SCHWANDER, G. FLAMANT and G. OLALDE
Institut de Science et de Génie des Matériaux et Procédés, U.P.R. du C.N.R.S., B.P. No. 5, Odeillo, 66120 Font-Romeu, France

(*Received* 24 *April* 1989 *and in final form* 23 *October* 1989)

Abstract—An original method for the calculation of transient temperature distribution in a semi-transparent non-scattering condensed medium accounting for radiation and conduction is presented. This method was developed in order to detail the influence of interface properties on temperature distribution. Diffuse and specular reflections of the walls for three situations (contact of the vitreous boundaries with the walls on both sides, any contact on both sides and contact on one side only) are compared for a grey medium. Large differences are shown for the latter case. Concerning the situation with any contact between walls and the STCM, a comparison between vitreous interfaces governed by Fresnel laws and diffuse vitreous interfaces is given. Significant differences are pointed out. For a glass layer the differences cannot be neglected, but they are reduced because of high absorptivity in the IR range.

INTRODUCTION

A GREAT deal of work has been reported concerning combined heat transfer in the following simplified situation: a semi-transparent non-scattering planar grey layer bounded by grey diffusely emitting and reflecting surfaces [1–4]. Subsequently, more realistic situations were examined in the field of non-scattering media. They are related to (i) the variation of optical properties with wavelength [5, 6], (ii) the nature of reflection at the boundary (specular reflection) [5], (iii) the mutual position of semi-transparent and opaque boundaries [7, 8]. Nevertheless, for one-dimensional systems, a general model taking into account most real situations is needed.

This paper presents a theoretical study of unsteady conductive and radiative heat transfer in a semi-transparent condensed material (STCM), accounting for: the variations of physical and optical properties of the medium with wavelength and temperature; the angular dependence of the reflection coefficient at the boundaries; the nature of reflection from the opaque boundaries; the position of the opaque wall with respect to the vitreous boundary.

Concerning the latter parameter, three situations have been examined according to the following considerations: the semi-transparent interfaces may be separated from the opaque boundary by a gap or may be in contact with it. The mutual position of both STCM boundaries and opaque walls leads to the three cases shown in Fig. 1.

(a) Conductive contact between the opaque wall and both STCM boundaries. A number of studies have been devoted to the analysis of heat transfer in this situation. The effects of the nature of reflection on the opaque wall on the temperature field have been examined by Timmons and Mingle [9] and Lii and Ozisik [10]; very small differences have been reported.

(b) No contact between opaque walls and the STCM boundaries. In this case the reflection at the vitreous boundary is governed by Fresnel laws. The results are less numerous than for the previous case. Stepanov *et al.* [7] have compared situations (a) and (b).

(c) Conductive contact on one STCM boundary and a non-conductive gap on the other side. Investigations concerning this situation are very poor. Some data are given by Marchenko *et al.* [8]. Significant temperature differences have been reported as a function of the nature of reflection.

In the first part of this paper the theoretical model and the numerical method are presented. The influence of the nature of reflection of the opaque wall on the temperature distribution in the STCM is then examined for the three cases (a), (b) and (c). Finally, results related to a glass layer in the third situation (c) are discussed.

THEORETICAL ANALYSIS

Mathematical formulation

We consider a flat layer of non-scattering semi-transparent condensed material of thickness Z_0 located between two specularly or diffusively reflecting surfaces of temperatures T_1 and T_2 ($T_1 > T_2$). These opaque boundaries may either be in contact with the vitreous interface (on one side or on both sides) or placed at some distance away from the layer. In the latter case the gap between the layer and the

NOMENCLATURE

C_p	specific heat
$E_n(x)$	$\int_0^1 \exp(-x/\mu)\mu^{n-2}\,d\mu$
I	intensity
I^0	black body intensity
K	number of directions μ_k
K_ν	spectral absorption coefficient
n	number of space intervals or total refractive index
n_ν	spectral refractive index
N	$\lambda K/4n^2\sigma T_1^3$
q	flux density
t	time
T	temperature
X	reduced space coordinate, $1-Z/Z_0$
Z	space coordinate
Z_0	depth of the medium.

Greek symbols

ε	emissivity
θ	reduced temperature, $(T-T_2)/(T_1-T_2)$
λ	thermal conductivity
μ_k	angular variable, $1 < k < K$ $(\mu = \cos\theta)$
ρ	density
σ	Stefan–Boltzmann constant
τ	optical depth, $\tau_\nu = K_\nu Z$
τ_0	optical thickness
ω_k	weight in the Gaussian formulation.

Subscripts

c	conductive
i	space index
I	spectral band, $\Delta\nu$
k	direction
r	radiative
1, 2	boundaries 1 and 2
+	hemisphere (+): $0 < \mu < 1$
−	hemisphere (−): $-1 < \mu < 0$.

Matrices

(E_I)	order K diagonal matrix
(I), (S), (G)	order K column matrices
(Id)	identity matrix
$(\rho_{j,I})$	order K square matrix related to the boundaries $j = 1, 2$.

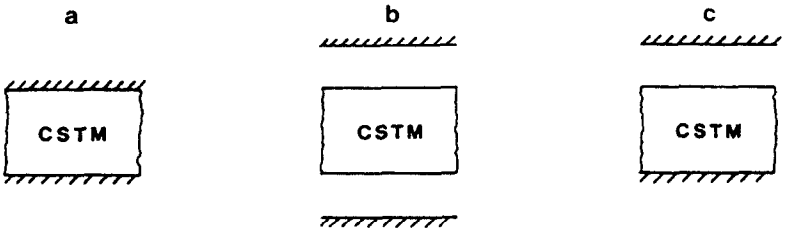

FIG. 1. Physical representation of the three situations occurring between walls and a vitreous medium layer.

wall is filled with a non-conductive medium with a refractive index of unity (Fig. 2).

At unsteady state the governing equations are

$$\rho C_p \frac{dT}{dt} = -\text{div}\,(\mathbf{q}_c + \mathbf{q}_r) \tag{1}$$

with

$$\text{div}\,\mathbf{q}_c = -\frac{\partial\lambda}{\partial T}\left(\frac{\partial T}{\partial Z}\right) - \lambda\frac{\partial^2 T}{\partial Z^2} \tag{2}$$

and

$$\text{div}\,\mathbf{q}_r = \int_0^\infty \text{div}\,\mathbf{q}_{r,\nu}\,d\nu =$$

$$2\pi\int_0^\infty \text{div}\left(\int_0^1 [I_\nu^+(Z,\mu) - I_\nu^-(Z,-\mu)]\mu\,d\mu\right)d\nu \tag{3}$$

where I_ν^+ and I_ν^- are the spectral intensities in the forward $(\mu > 0)$ and backward $(\mu < 0)$ directions. The spectral radiative flux $\mathbf{q}_{r,\nu}$ may be expressed as

$$\text{div}\,(\mathbf{q}_{r,\nu}) = \kappa_\nu\left[4\pi n_\nu^2 I_\nu^0(T(\tau))\right.$$

$$\left. -2\pi\left[\int_0^1 I_\nu^+(0,\mu)\exp(-\tau/\mu)\,d\mu\right.\right.$$

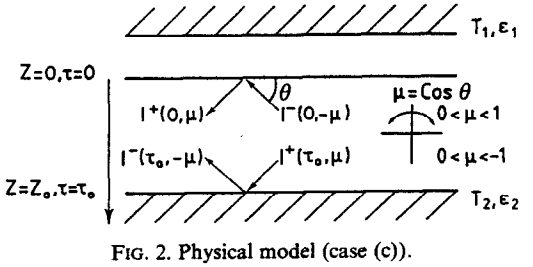

FIG. 2. Physical model (case (c)).

$$+\int_0^1 I_\nu^-(\tau_{0,\nu},-\mu)\exp\left[-(\tau_{0,\nu}-\tau)/\mu\right]\mathrm{d}\mu$$

$$+n_\nu^2\int_0^\tau I_\nu^0(T(\tau'))E_1(\tau-\tau')\,\mathrm{d}\tau'$$

$$+n_\nu^2\int_\tau^{\tau_{0,\nu}} I_\nu^0(T(\tau'))E_1(\tau'-\tau)\,\mathrm{d}\tau'\Big]\Big] \quad (4)$$

where

$$\tau_\nu=\int_0^z K_\nu(T)\,\mathrm{d}z$$

(K_ν is the spectral absorption coefficient), I_ν^0 the Planck function and

$$E_1(x)=\int_0^1 \exp(-x/\mu)\mu^{-1}\,\mathrm{d}\mu.$$

For a given temperature profile $T(Z)$, the spectral intensities at the boundaries $\tau=0$, $I_\nu^+(0,\mu)$ and $\tau=\tau_0$, $I_\nu^-(\tau_{0,\nu},-\mu)$ are solutions of the general boundary conditions

$$I_\nu^+(\tau_{0,\nu},\mu)=I_\nu^+(0,\mu)\exp(-\tau_{0,\nu}/\mu)$$

$$+n_\nu^2\int_0^{\tau_{0,\nu}}\frac{I_\nu^0(T(\tau))}{\mu}\exp\left[-(\tau_{0,\nu}-\tau)/\mu\right]\mathrm{d}\tau \quad (5)$$

$$I_\nu^-(0,-\mu)=I_\nu^-(\tau_{0,\nu},-\mu)\exp(-\tau_{0,\nu}/\mu)$$

$$+n_\nu^2\int_0^{\tau_{0,\nu}}\frac{I_\nu^0(T(\tau))}{\mu}\exp(-\tau/\mu)\,\mathrm{d}\tau \quad (6)$$

$$I_\nu^+(0,\mu)=\int_0^1\rho_\nu^1(\mu,\mu')I_\nu^-(0,-\mu')\,\mathrm{d}\mu'+G_\nu^1(\mu) \quad (7)$$

$$I_\nu^-(\tau_0,-\mu)=\int_0^1\rho_\nu^2(\mu,\mu')I_\nu^+(\tau_0,\mu')\,\mathrm{d}\mu'+G_\nu^2(\mu). \quad (8)$$

The functions $\rho_\nu^i(\mu,\mu')$ and $G_\nu^i(\mu)$ ($i=1$ and 2) are related to the nature of reflection at boundaries 1 and 2 and to the type of contact with the vitreous interface and the opaque wall.

Numerical solution

Previous numerical works about heat transfer in condensed semi-transparent media may be examined from the boundaries properties point of view.

Diffuse reflection from the opaque wall. The angular variation of the spectral intensity can be ignored when solving the equations. The theoretical studies of Heaslet and Warming [11], Viskanta [12] and Hottel and Sarofim [13] are related to this assumption. The zoning method [13] was extended to problems with constant specular reflection by Eckert and Sparrow [14]. Nevertheless, this method seems to be invalid for modelling complex boundaries.

Angular variation of properties at the boundaries (wall and vitreous interface). Various numerical methods have been developed: the spherical harmonics method, the moment method, the normal modes method [15], the discrete ordinates method [16] and the Monte Carlo method [17].

The discrete ordinate method appears to be most commonly adopted for complex boundary conditions. For example, where Fresnel reflection is concerned, the hemisphere may be divided into several sectors in order to take into account the angular variation of the reflection coefficient [7] (Fig. 3). In addition, a Gaussian quadrature is generally used to perform the angular integration of the radiation intensity. Among previous works in this field, two numerical techniques were proposed: (i) numerical solution of the radiation transfer equation by superposition of the homogeneous solutions satisfying the boundary conditions on the intensities [5]; (ii) numerical solution of the expanded equations, consisting of the development of integration procedures. We chose the latter solution.

The integration of (1) with respect to time t is performed using the implicit finite difference Crank–Nicolson method. Concerning the space coordinate, a variable interval grid is used.

Methods for integrating equation (3) with respect to wavelength angle and optical coordinate are the following.

(1) *Wavelength.* The spectral variation of the absorption coefficient is introduced using a band model. If we define M bands (index I), equations (4)–(8) may be formulated on each band by substitution of index I for ν, and equation (3) can then be expressed as

$$\operatorname{div}\mathbf{q}_r=\sum_{I=1}^{M}\operatorname{div}\mathbf{q}_{r,I}. \quad (9)$$

(2) *Angular direction.* A fixed number (K) of discrete directions (μ_k) is considered and the directional integrals are replaced by weighted sums according to a Gaussian formulation

$$\int_{\mu\in\Delta\mu}f(\mu)\,\mathrm{d}\mu=\sum_{\mu_k\in\Delta\mu}\omega_k f(\mu_k). \quad (10)$$

(3) *Optical coordinate.* The optical thicknesses $\tau_1,\ldots,\tau_i,\ldots,\tau_N$ correspond to the space coordinates $Z_1,\ldots,Z_i,\ldots,Z_N$. The integration of equations such as

$$\int_0^{\tau_{0,I}}\{I_I^0[T(\tau)]\exp(-\tau/\mu)/\mu\}\,\mathrm{d}\mu$$

are performed on the basis of a linear approximation of $L_I^0[T(\tau)]$. Concerning integrals

$$\int_0^{\tau_{0,I}}n_I^2 I_I^0[T(\tau')]E_1(|\tau-\tau'|)\,\mathrm{d}\tau'$$

the approximations are shown in Fig. 4. In order to perform the integration at $\tau=\tau_i$, L_I^0 is expressed as a linear function of τ at any point of the grid except for $\tau=\tau_i$, where a second order polynomial approxi-

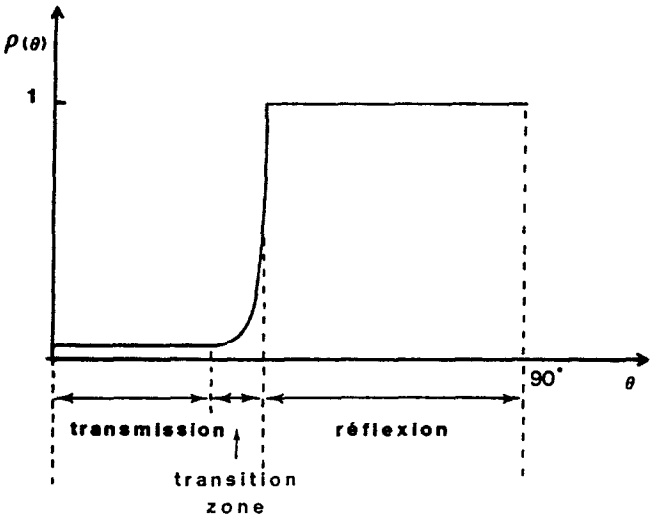

FIG. 3. Reflection of radiation on an ideal vitreous interface.

mation is introduced. For $\tau = 0$ and $\tau = \tau_0$ (boundaries), a linear approximation is used.

Numerical procedure

At time t, $\mathbf{q}_{r,I}$ is calculated according to the following steps.

Calculation of intensities at the interfaces. The matrix formulation of equations (5) and (6) may be written as

$$(I_I^+(\tau_{0,I})) = (E_I)(I_I^+(0)) + (S_I^+) \quad (5a)$$

$$(I_I^-(0)) = (E_I)(I_I^-(\tau_{0,I})) + (S_I^-) \quad (6a)$$

where (E_1) is a diagonal K order matrix, the diagonal elements of which are $\exp(-\tau_{0,I}/\mu_k)$; (S_I^+) and (S_I^-) are vectors corresponding to the integrals of equations (5) and (6). The discrete expressions of S_I^+ and S_I^- are developed in Appendix A.

The matrix formulations of equations (7) and (8) are

$$(I_I^+(0)) = (\rho_{1,I})(I_I^-(0)) + (G_{1,I}) \quad (7a)$$

$$(I_I^-(\tau_{0,I})) = (\rho_{2,I})(I_I^+(\tau_{0,I})) + (G_{2,I}). \quad (8a)$$

The elements of square K order matrix $(\rho_{i,I})$ and column matrix $(G_{i,I})$ are given by the boundary properties. Taking into account the relations (5a)–(8a), two K order linear systems are deduced and solved to determine $(I_I^+(0))$ and $(I_I^-(\tau_{0,I}))$ in order to calculate div $\mathbf{q}_{r,I}$.

The following K order linear system is obtained:

$$[(Id) - (\rho_{1,I})(E_I)(\rho_{2,I})(E_I)](I_I^+(0)) = (\rho_{1,I})(S_I^-) + (G_{1,I}) + (\rho_{1,I})(E_I)[(\rho_{2,I})(S_I^+) + (G_{2,I})] \quad (7b)$$

$$[(Id) - (\rho_{2,I})(E_I)(\rho_{1,I})(E_I)](I_I^-(\tau_{0,I})) = (\rho_{2,I})(S_I^+) + (G_{2,I}) + (\rho_{2,I})(E_I)((\rho_{2,I})(S_I^-) + (G_{1,I})). \quad (8b)$$

Calculation of div $\mathbf{q}_{r,I}$. This calculation is performed on the basis of equation (4) expressed on a band I. It takes into account the intensities at the boundaries:

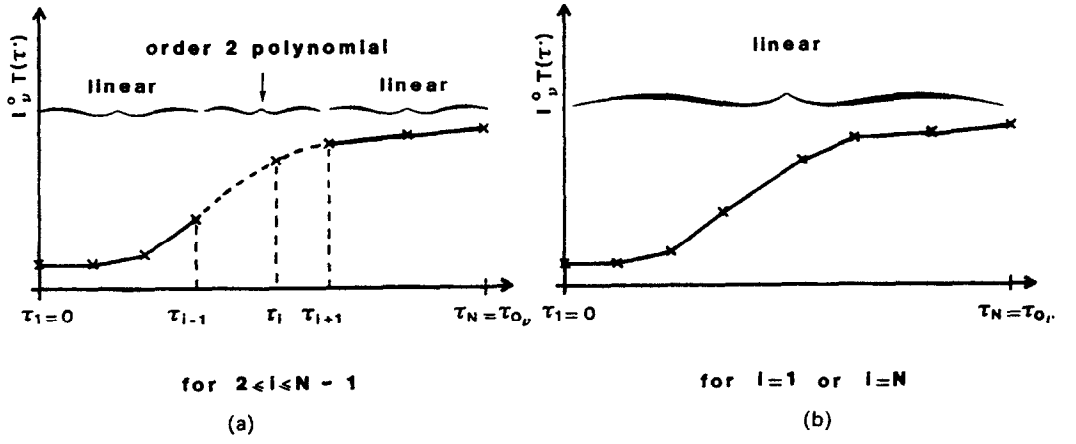

FIG. 4. Schematic of the space integration method.

Table 1. Situations described by the model

	Core of the STCM				Boundaries		
Variable	t	T	ν	μ	T	ν	μ
General formulation	yes	—	yes	yes	Contact or no contact with walls		
Parameters							
K_ν	—	yes	yes	—			
n_ν	—	yes	yes	—			
ρ, C_p, λ	—	yes	—	—			
t_i, ρ_{ij}, ε_{ij}	—	—	—	—	yes	yes	yes

$I_i^+(0)$ and $I_i^-(\tau_{0,i})$ and the temperature distribution (using the Planck function; Appendix A).

Model performances and limitations

The situations described by the previously formulated model are listed in Table 1. Most of the real situations encountered when studying heat transfer in condensed one-dimensional semi-transparent materials may be examined by this model.

The numerical solution proposed in this paper is original and may be compared with the zonal method, both being adapted for calculations using a variable mesh grid. Nevertheless, some limitation of the latter method is illustrated in the case of optically thick material.

Let us consider a grey medium divided into a finite number of elements ΔZ so that $\Delta\tau = K\Delta Z \gg 1$. At any point of the medium, the divergence of the radiative flux is expressed as

zonal method:

$$\operatorname{div} \mathbf{q}_r(\mathbf{Z}_i) = -n^2\sigma\frac{T^4(Z_{i+1})-2T^4(Z_i)+T^4(Z_{i-1})}{\Delta Z}$$

this method:

$$\operatorname{div} \mathbf{q}_r(\mathbf{Z}_i) = -\frac{4}{3K}n^2\sigma\frac{T^4(Z_{i+1})-2T^4(Z_i)+T^4(Z_{i-1})}{(\Delta Z)^2}.$$

It may be noticed that the second formulation is in agreement with Rosseland's approximation. This difference between the two methods is due to the approximation on I^0 in the vicinity of Z_i (internal ΔZ). For the zonal method, $I^0(Z_i)$ is constant for $Z_i-\Delta Z/2 \leqslant Z_i \leqslant Z_i+\Delta Z/2$; for the present method $I^0(Z_i)$ is expressed as a second order polynomial in the same range.

This observation is illustrated in Fig. 5. As pointed out by Kunc [18], the accuracy of the calculations by the zonal method depends on the optical depth $\Delta\tau_i$: for $\Delta\tau_i > 0.2$, the numerical error in the intensity calculation increases with $\Delta\tau_i$. For example, it reaches 4% for $\Delta\tau_i = 0.5$. For $\Delta\tau_i \leqslant 0.2$ no difference between exact and numerically calculated intensities is observed.

In the case of pure radiative transfer or strong absorption at the boundary, a fine discretization is needed to obtain a good representation of the temperature profile's local shape.

In order to compare the present numerical solution with previous results, calculated values of the temperature distribution are listed in Table 2 for the example proposed by Saulnier [4]: a grey medium in contact with two black walls at temperature $T_1 = 500$ K and $T_2 = 300$ K, respectively (in addition $\lambda = 0$ and $\tau_0 = 1$). Our results [19], obtained by dividing each hemisphere in ten directions, are compared with data published by Heaslet and Warming [11] and Saulnier [4] for two grids. Results are in good agreement:

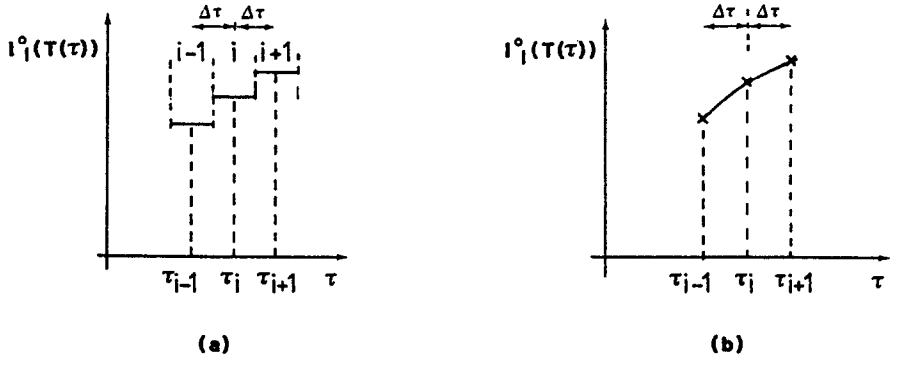

FIG. 5. Representation of I^0 at the mode τ_i. (a) Zonal method. (b) This method.

Table 2. Numerical solution comparison

X	Heaslet and Warming [11]	Saulnier [4] (23 nodes)	This study (11 points)	Saulnier [4] (103 nodes)	This study (101 points)
0	382.36	382.85	381.68	382.04	381.80
0.1	395.75	396.42	396.19	396.49	396.50
0.2	406.70	407.29	407.16	407.32	407.30
0.3	417.57	416.78	416.69	416.78	416.76
0.4	424.67	425.41	425.36	425.41	425.39
0.5	433.75	433.45	433.43	433.45	433.43
0.6	441.73	441.06	441.08	441.06	441.05
0.7	447.76	448.39	448.44	448.39	448.38
0.8	456.01	455.56	455.63	455.56	455.54
0.9	463.29	462.84	462.99	462.82	462.79
1.0	471.03	470.87	471.36	471.21	471.29

Grey medium, $T_1 = 500$ K, $T_2 = 300$ K, $\tau_0 = 1$. This study: ten directions on each hemisphere.

temperature differences less than 0.2 K are observed (generally 2×10^{-2} K) for about 100 intervals. It may be noticed that the present method gives roughly the same precision as the nodal method, using a smaller number of intervals.

RESULTS

The model is illustrated for two media: a grey medium (ideal case) and a glass (real case).

1. *Grey medium*

Influence of the interface configurations on temperature profiles. The three mutual positions of the semi-transparent material with respect to the opaque walls are described in Fig. 1. Typical temperature profiles related to these configurations are illustrated in Fig. 6 for diffuse black walls and dominant radiative transfer ($N = 0.005$). The representation is dimensionless: $\theta = (T-T_2)/(T_1-T_2)$ is plotted as a function of the depth $X = 1-Z/Z_0$. T_1 is the temperature of the hottest wall (right-hand side of the figure). The dimensionless time t^* is defined as $t^* = at/Z_0^2$ with $a = \lambda/\rho C_p$ and the medium is supposed to be at temperature T_2 at time $t = 0$.

When contact between walls and vitreous interfaces occurs on both sides (Fig. 6(a)), the temperature profile exhibits an S-shape as expected. For the opposite situation (no contact), the profile is nearly linear (Fig. 6(b)). The influence of contact on the transient behaviour is noticeable. Steady state is observed more rapidly when the wall is in contact with the vitreous material: steady state is reached for $t^* = 1.9$ for case (a) and $t^* = 2.8$ for case (b).

Effect of the boundary properties on temperature profiles—optical properties of the wall. Two situations have been compared: specular and diffuse reflections on the opaque boundaries for three configurations (Fig. 1).

Concerning the two configurations, contact or no contact with the walls on both sides of the STCM, our results are in agreement with the conclusions proposed by Timmons and Mingle [9], Lii and Ozisik [10] and Anderson and Viskanta [5]: the influence of the wall reflection type may be neglected either during transient heating or steady state conditions whatever the values of the optical depth and refractive index.

This conclusion is modified when considering the configuration (c) in Fig. 1: direct contact of the vitreous medium with the wall on one side only. First, concerning the side without any contact, the effect of the reflection character of the wall or of the vitreous interface may be neglected. However, on the other side, significant differences are proved. Transient (t_1^*, t_2^*) and steady state (t_3^*) temperature profiles are plotted in Fig. 7 for three values of the optical depth, τ_0. Dotted and solid lines relate to a diffuse or a constant specular reflection of wall 2 respectively. The differences between temperature distributions are important for both transient and steady state conditions and they increase when the optical depth decreases. The interaction conduction-to-radiation parameter N proves to have some effect on the general shape of the curves but no variation of the differences between the profiles has been noticed.

Optical properties of vitreous interfaces. In this part of the work no kind of contact between the walls and the STCM is supposed to occur and two types of transparent boundary are compared (see Fig. 8).

(a) An ideal vitreous boundary whose properties are determined by the Fresnel laws and the refractive index of the medium.

(b) An isotropic diffuse boundary whose optical properties (reflectivity, transmittivity, emissivity) are diffuse and isotropic. In this case the whole radiative properties of the boundary are defined if one of the factors and the refractive index are known (hemispherical transmittivity air-to-glass $= n^2 \cdot$ hemispherical transmittivity glass-to-air). They are calculated on the basis of the hemispherical properties of the vitreous interface corresponding to an isotropic incident intensity (Fig. 8).

The advantages of this latter approach are, first, it

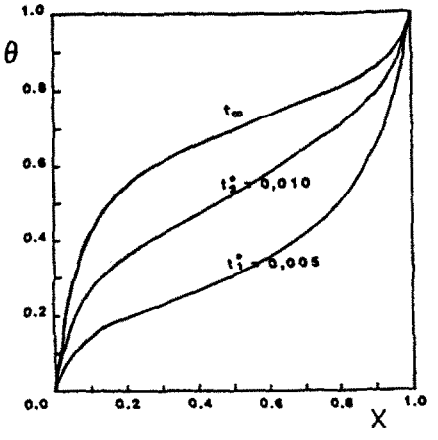

(a)

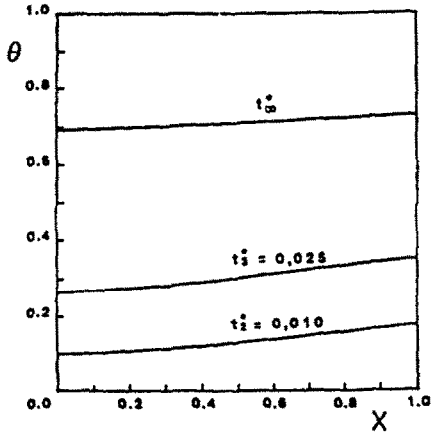

(b)

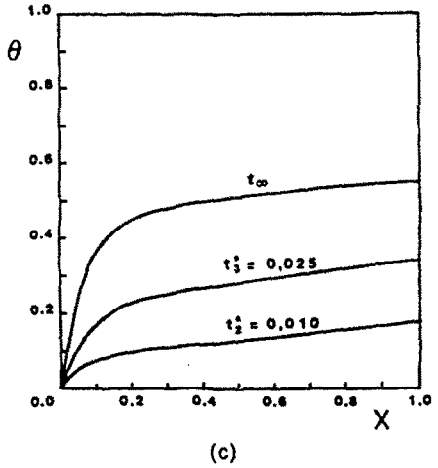

(c)

FIG. 6. Typical transient temperature profile in a grey medium as a function of the boundary configuration. (a), (b), (c): see Fig. 1. $n = 2$, $N = 0.005$, $\varepsilon_1 = \varepsilon_2 = 1$.

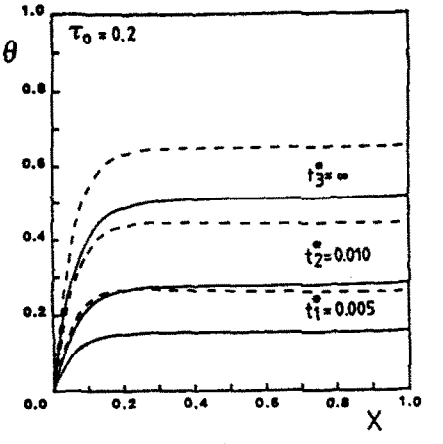

(a)

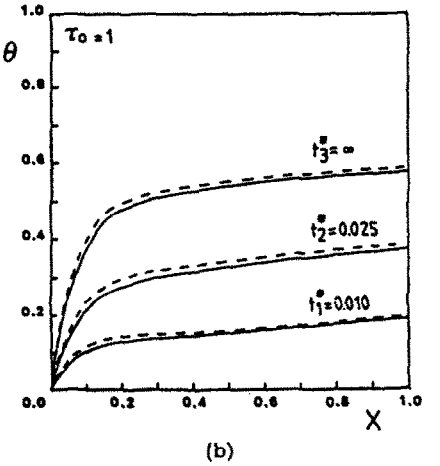

(b)

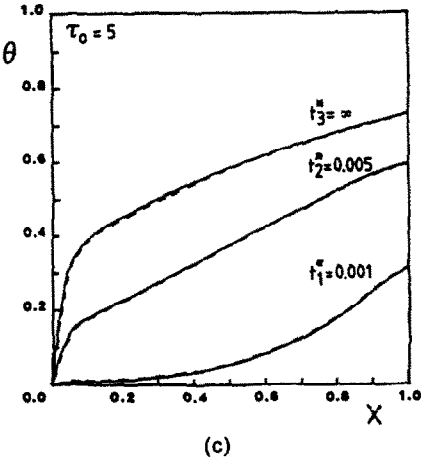

(c)

FIG. 7. Effect of the type of reflection on the transient temperature profile as a function of the optical thickness. Configuration (c). $n = 2$, N/τ_0^2 ($\tau_0 = 0.1$) or $N = 5 \times 10^{-3}$ ($\tau_0 = 1$ and 5), $\varepsilon_1 = 1$, $\varepsilon_2 = 0.21$.

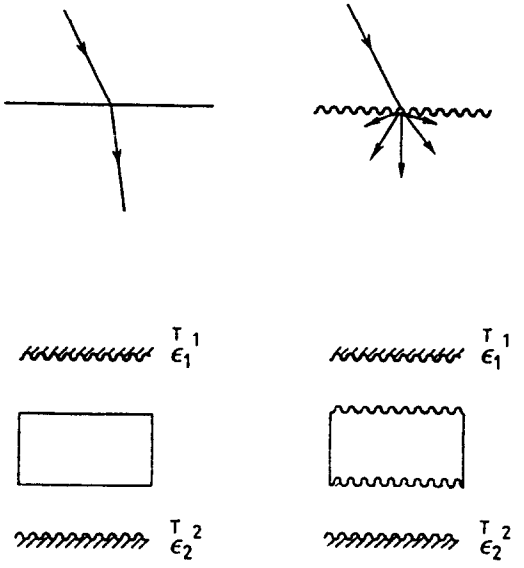

FIG. 8. Physical model of the isotropic diffuse boundary.

is an easy approximation for examining the influence of non-ideal vitreous boundaries on temperature distribution (roughness, for example). Second, it is a mathematical equivalence in the model (the calculations are simplified) and it is useful to define the range of parameters for which this equivalence may be used.

In Fig. 9, the calculated temperature profiles for both previous cases are compared as a function of the optical depth. The differences between the ideal vitreous boundary and the isotropic diffuse boundary decrease when the optical depth and the time increase. Temperature differences become very small for $\tau_0 > 5$ and at steady state. No change of this conclusion is observed as a function of N.

2. *Molten glass bath*

Previous illustration proves that significant modifications of the temperature distribution are predicted inside a grey STCM in contact with a black wall on one side when the type of reflection of this wall is modified (diffuse or specular). The objective of this section is to examine the same problem for a real medium such as molten glass.

The temperature distribution inside a 1 cm, 2 cm and 5 cm deep molten glass layer is illustrated in Fig. 10 for the following conditions: bottom wall, $T_2 = 1200$ K, $\varepsilon_2 = 0.21$; upper wall, $T_1 = 1500$ K, $\varepsilon_1 = 1$. Thermophysical properties of the glass are detailed in Appendix B. A four-band model is used to describe the variation of K_ν with wavelength. When changing the reflection type of the bottom, the temperature differences are less significant than observed for the grey medium, but they do exist. This observation is due to the strong absorption of IR radiation at the layer surface ($K_\nu \to \infty$ for $\lambda \geqslant 4$ μm).

Another illustration of this model is given in Fig. 11. The temperature distribution in a 25 cm deep bath is plotted at steady state with the bottom emissivity (ε_2) as the parameter (diffuse reflection is assumed). It may be noticed that the free boundary temperature is almost affected by the change of ε_2 but the thermal

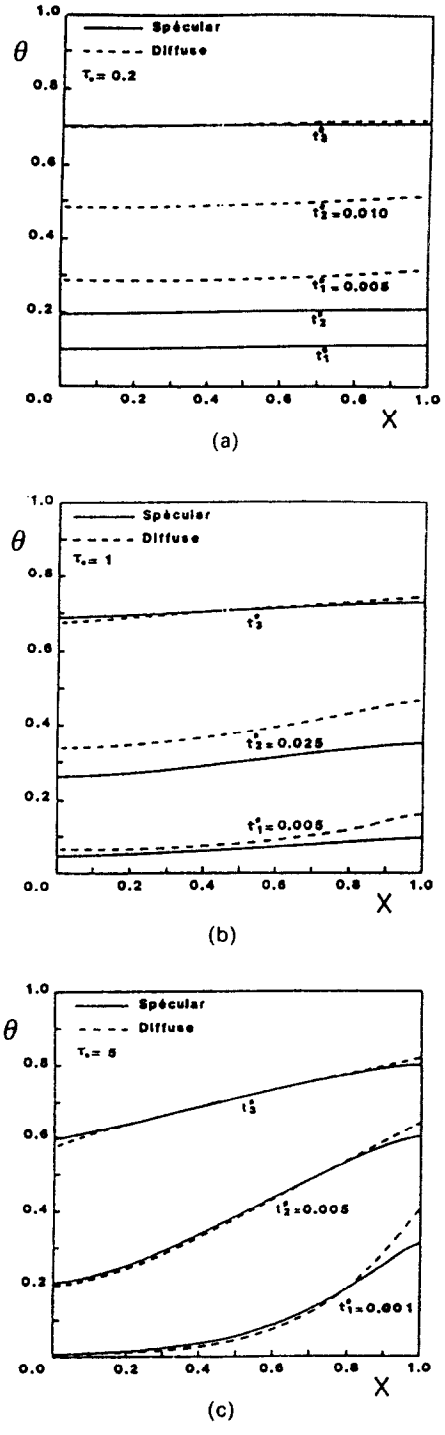

FIG. 9. Comparison of ideal vitreous interfaces and isotropic diffuse vitreous boundaries. Configuration (b). $n = 2$, N/τ_0^2 ($\tau_0 = 0.2$) or $N = 5 \times 10^{-3}$ ($\tau_0 = 1$ and 5), $T_1/T_2 = 2$, $\varepsilon_1 = \varepsilon_2 = 1$.

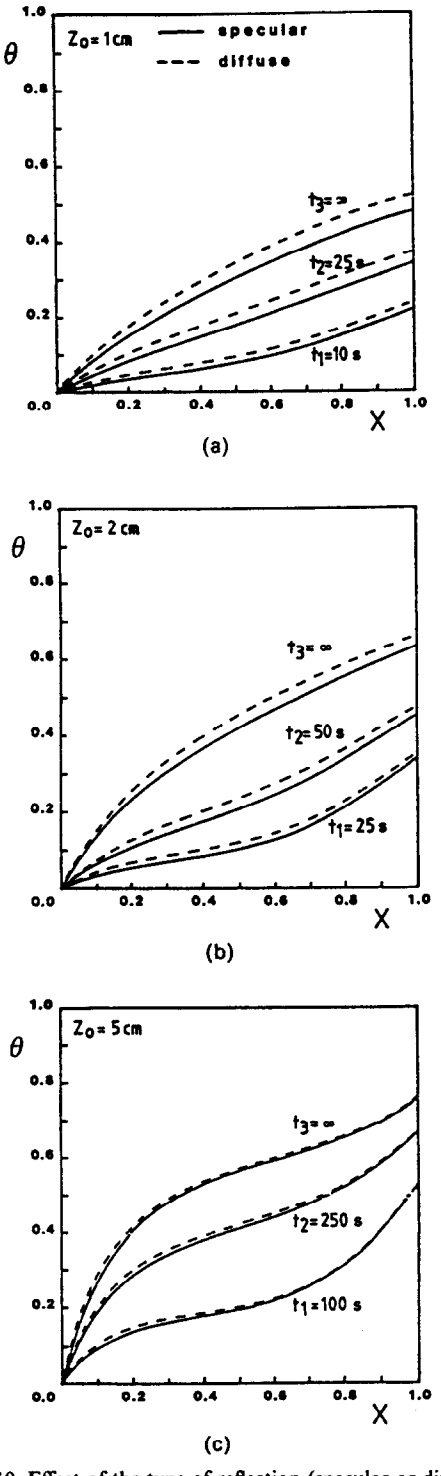

FIG. 10. Effect of the type of reflection (specular or diffuse) on the transient temperature profile in glass as a function of the depth. $n = 1.52$, $T_1 = 1500$ K, $T_2 = 1200$ K, $\varepsilon_1 = 1$, $\varepsilon_2 = 0.21$, t_j are real times in seconds. Configuration (c).

gradient (heat flux) at $Z = 0$ exhibits large variations: it reaches 10^4 K m^{-1} for $\varepsilon_2 = 0$ and 4×10^3 K m^{-1} for $\varepsilon_2 = 1$. The consequence of this observation on heat transfer through the wall is very important.

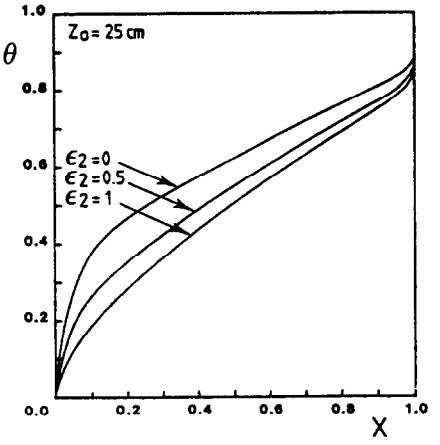

FIG. 11. Influence of the bottom emissivity on the steady state temperature distribution in a 25 cm deep molten glass layer. Configuration (c).

CONCLUSION

A general formulation and numerical solution of heat transfer in STCM is proposed in order to examine various interface configurations. The more significant results are the following.

When both interfaces of a vitreous grey material are in contact or without any contact with the opaque walls on both sides the temperature difference calculated when changing the type of reflection on the walls (specular or diffuse) may be neglected. For the latter configuration (no contact) the temperature distribution is modified when the vitreous boundary properties are changed.

If only one side of the grey STCM is in contact with a wall, the temperature distribution is affected by a modification of the type of this side reflection. The differences decrease when the optical depth of the medium increases.

The previous conclusions also hold for a glass layer but the differences are smaller due to the strong absorption of IR radiation at the glass surface.

REFERENCES

1. R. Viskanta and R. J. Grosh, Heat transfer by simultaneous conduction and radiation in an absorbing medium, *Trans. ASME, J. Heat Transfer* **84**, 63–73 (1962).
2. K. Prasad and R. J. Hering, Transient radiative heat transfer in a planar layer, *Int. J. Heat Mass Transfer* **12**, 1331–1337 (1969).
3. D. G. Doornink and R. G. Hering, Transient combined conductive and radiative heat transfer, *Trans. ASME, J. Heat Transfer* Nov., 473–478 (1972).
4. J. B. Saulnier, La modélisation thermique et ses applications aux transferts couplés et au contrôle actif, Thesis, Université de Poitiers (1980).
5. E. E. Anderson and R. Viskanta, Spectral and boundary effects on coupled conduction–radiation heat transfer through semi-transparent solids, *Wärme- und Stoffübertr.* **1**, 14–24 (1973).
6. T. Kunc, M. Lallemand and J. B. Saulnier, Some new developments on coupled radiative–conductive heat

transfer in glasses: experiments and modeling, *Int. J. Heat Mass Transfer* **27**, 2307–2319 (1984).
7. S. V. Stepanov, V. A. Petrov and V. K. Bityukov, Radiative–conductive heat transfer in a flat layer of a selective medium with semi-transparent boundaries, *High Temp.* (1979), translated from *Teplof. Vys. Temp.* **16**(6), 1277–1284 (1978).
8. N. V. Marchenko, B. I. Aronov and Ya. I. Shtipel'man, Calculation of unsteady radiative–conductive heat transfer in a plane layer of selective medium with semi-transparent boundaries, *High Temp.*, translated from *Teplof. Vys. Temp.* **18**(5), 1007–1017 (1980).
9. D. H. Timmons and J. O. Mingle, Simultaneous radiation and conduction with specular reflection, AIAA Paper No. 68-28 (1968).
10. C. C. Lii and M. N. Ozisik, Transient radiation and conduction in an absorbing emitting, scattering slab with reflective boundaries, *Int. J. Heat Mass Transfer* **15**, 1175–1179 (1972).
11. M. A. Heaslet and R. Warming, Radiative transport and wall temperature slip in an absorbing planar medium, *Int. J. Heat Mass Transfer* **8**, 979–994 (1965).
12. R. Viskanta, Heat transfer by conduction and radiation in absorbing and scattering materials, *Trans. ASME, J. Heat Transfer* **Feb.**, 143–150 (1965).
13. H. C. Hottel and A. F. Sarofim, *Radiative Transfer*. McGraw-Hill, New York (1967).
14. E. R. G. Eckert and E. M. Sparrow, Radiative heat exchange between surfaces with specular reflection, *Int. J. Heat Mass Transfer* **3**, 42–54 (1961).
15. M. N. Ozisik, *Radiative Transfer and Interactions with Conduction and Convection*. Wiley–Interscience, New York (1973).
16. S. Chandrasekhar, *Radiative Transfer*. Dover, New York (1960).
17. A. Al Abed and J. F. Sacadura, A Monte Carlo finite difference method for coupled radiation–conduction heat transfer in semitransparent media, *Trans. ASME, J. Heat Transfer* **105**, 931–933 (1983).
18. T. Kunc, Etude du transfert couplé conduction–rayonnement, application à la détermination de la conductivité phonique des verres à haute température par identification paramétrique. Thesis, Université de Poitiers, France (1984).
19. D. Schwander, Influence des propriétés radiatives des interfaces sur les transferts thermiques dans les milieux semi-transparents condensés. Thesis, Université de Perpignan (1988).
20. C. Ades, T. Toganidis and J. P. Traverse, High temperature optical spectra of glasses and modelization in view of energetic applications, Int. Congress on Glass, Leningrad, U.S.S.R., 2–7 July (1989).

APPENDIX A. DEVELOPMENT OF EQUATIONS FOR THE CALCULATION OF div $\mathbf{q}_{r,l}(\mathbf{Z}_i)$

The expressions of the elements of the vectors S_l^+ and S_l^- are as follows:

$$S_{l,k}^+ = n_l^2 \int_0^{\tau_{0,l}} \mu_k^{-1} I_l^0(\tau) \exp\left(-(\tau_{0,l}-\tau)/\mu_k\right) \mathrm{d}\tau$$

$$\equiv n_l^2 \left[I_l^0(\tau_{0,l}) - I_l^0(0) \exp\left(-\tau_{0,l}/\mu_k\right) - \sum_{i=1}^{N-1} \frac{I_l^0(\tau_{i+1}) - I_l^0(\tau_i)}{\tau_{i+1}-\tau_i} \mu_k \exp\left(-\frac{\tau_{0,l}-\tau_{i+1}}{\mu_k}\right) \times \left(1-\exp\left[-(\tau_{i+1}-\tau_i)/\mu_k\right]\right) \right]$$

$$S_{l,k}^- = n_l^2 \int_0^{\tau_{0,l}} \mu_k^{-1} I_l^0(\tau) \exp\left(-\tau/\mu_k\right) \mathrm{d}\tau$$

$$\equiv n_l^2 \left[I_l^0(0) - I_l^0(\tau_{0,l}) \exp\left(-\tau_{0,l}/\mu_k\right) + \sum_{i=1}^{N-1} \frac{I_l^0(\tau_{i+1}) - I_l^0(\tau_i)}{\tau_{i+1}-\tau_i} \mu_k \exp\left(-\tau_i/\mu_k\right) \times \left(1-\exp\left[-(\tau_{i+1}-\tau_i)/\mu_k\right]\right) \right].$$

This becomes

$$\operatorname{div} \mathbf{q}_{r,l}(\mathbf{Z}_i) = -2\pi K_l \left[\sum_{k=1}^{K} \omega_k [I_l^+(0,\mu_k) - n_l^2 I_l^0(T(0))] \times \exp\left(-\tau_i/\mu_k\right) + \sum_{k=1}^{K} \omega_k [I_l^-(\tau_{0,l},-\mu_k) - n_l^2 I_l^0(T(\tau_{0,l}))] \exp\left[-(\tau_{0,l}-\tau_i)/\mu_k\right] + n_l^2 [F_1(\tau_i) + F_2(\tau_i)] \right]$$

with

$$F_1(\tau_i) = \sum_{j=1}^{N-1} [I_l^0(\tau_{j+1}) - I_l^0(\tau_j)] \frac{E_3(|\tau_j-\tau_i|) - E_3(|\tau_{j+1}-\tau_i|)}{\tau_{j+1}-\tau_j}$$

$F_2(\tau_i) = 0$ if $\tau_i = 0$ and $\tau_i = \tau_{0,l}$

$$F_2(\tau_i) = \frac{2}{\tau_{i+1}-\tau_{i-1}} \left[\frac{I_l^0(\tau_{i+1}) - I_l^0(\tau_i)}{\tau_{i+1}-\tau_i} + \frac{I_l^0(\tau_{i-1}) - I_l^0(\tau_i)}{\tau_i - \tau_{i-1}} \right] \cdot \left[\frac{1}{3}\left[1-\exp\left(-[\tau_i-\tau_{i-1}]\right)\right] - \frac{1}{6}(\tau_i-\tau_{i-1}) E_3(\tau_i-\tau_{i-1}) - \frac{\tau_i-\tau_{i-1}}{4} + \frac{1}{3}\left[1-\exp\left(-[\tau_{i+1}-\tau_i]\right)\right] - \frac{1}{6}(\tau_{i+1}-\tau_i) E_3(\tau_{i+1}-\tau_i) - \frac{\tau_{i+1}-\tau_i}{4} \right].$$

APPENDIX B. THERMOPHYSICAL PROPERTIES OF GLASS

For calculations, the following properties have been used:

$$\lambda = 0.93 + 8 \times 10^{-4} T \ (\mathrm{W\ m^{-1}\ K^{-1}})$$

$$\rho = 2.4 \times 10^3 \ \mathrm{kg\ m^{-3}}$$

$$C_p = 1.17 \times 10^3 \ \mathrm{J\ kg^{-1}\ K^{-1}}.$$

The variation of K_ν with wavelength is a simplified representation of the band model developed by Ades *et al.* [20]. It is listed in Table B1.

Table B1. K_ν vs λ

$0.4 < \lambda < 2.72\ \mu\mathrm{m}$	$K_\nu = 16\ \mathrm{m^{-1}}$, $T = 1200$ K $K_\nu = 21\ \mathrm{m^{-1}}$, $T = 1500$ K
$2.72 < \lambda < 4.37\ \mu\mathrm{m}$	$K_\nu = 450\ \mathrm{m^{-1}}$, $1200 < T < 1500$ K
$\lambda > 4.37\ \mu\mathrm{m}$	$\varepsilon_\nu = 1$

$n_\nu = 1.52$.

INFLUENCE DES PROPRIETES DES INTERFACES SUR LA DISTRIBUTION TRANSITOIRE DE TEMPERATURE DANS UN MILIEU SEMITRANSPARENT CONDENSE NON DIFFUSANT

Résumé—Une méthode originale de calcul du profil de température en régime dynamique dans un milieu semi transparent non diffusant condensé est présenté. La méthode est destinée à l'examen théorique détaillé de l'influence des propriétés des interfaces sur le profil de température. On compare les distributions obtenues avec des parois à réflexion diffuse et spéculaire dans trois configurations: contact direct des interfaces vitreuses avec les parois, aucun contact, contact sur une face seulement. Dans le cas d'un milieu gris, des différences notables sont mises en évidence pour la dernière configuration d'interfaces. Les distributions de température obtenues à partir d'interfaces vitreuses pour deux types de propriétés, règles de Fresnel—propriétés diffuses, dans le cas d'une configuration sans contact sont également comparés. Des différences significatives sont mises en évidence. Dans le cas d'une couche de verre, les mêmes différences sont observées mais de façon moins accentuée à cause de l'opacité du verre au delà de 4 μm.

EINFLUSS DER GRENZFLÄCHENEIGENSCHAFTEN AUF DIE TRANSIENTEN TEMPERATURVERTEILUNGEN IN KONDENSIERTEN HALBDURCHLÄSSIGEN MEDIEN

Zusammenfassung—Es wird ein neues Verfahren für die Berechnung der transienten Temperaturverteilung in einem halbdurchlässigen nichtstreuenden kondensierten Medium vorgeschlagen, das sowohl Strahlung als auch Leitung berücksichtigt. Das Verfahren wurde entwickelt, um den Einfluß der Grenzflächeneigenschaften auf die Temperaturverteilung detailliert zu untersuchen. Die diffuse und die Gesamtreflexion der Wände werden für ein graues Medium und drei Situationen verglichen: Kontakt der gläsernen Oberflächen mit den Wänden an beiden Seiten, kein Kontakt und Kontakt an nur einer Seite. Im letzten Fall ergeben sich große Unterschiede. Für den Fall, bei dem kein Kontakt zu den Wänden besteht, wird ein Vergleich zwischen gläsernen Oberflächen, die den Fresnel-Gesetzen gehorchen, und diffusen Oberflächen angestellt. Wichtige Unterschiede werden dabei aufgezeigt. Für eine Glasschicht können die Unterschiede nicht vernachlässigt werden, aber man kann sie durch das große Absorptionsvermögen im Infrarotbereich reduzieren.

ВЛИЯНИЕ ГРАНИЧНЫХ СВОЙСТВ НА НЕСТАЦИОНАРНОЕ РАСПРЕДЕЛЕНИЕ ТЕМПЕРАТУР В КОНДЕНСИРОВАННЫХ ПОЛУПРОЗРАЧНЫХ СРЕДАХ

Аннотация—Предложен оригинальный метод расчета нестационарного распределения температур в полупрозрачной нерассеивающей конденсированной среде, учитывающий излучение и теплопроводность. Метод разработан с целью уточнения влияния свойств межфазной границы на распределение температур. Выполнено сравнение диффузного и зеркального отражений стенок для серой среды в трех случаях. Проведено сравнение стекловидных межфазных границ при выполнении закона Френеля и при диффузном отражении в случае любого контакта между стенками и полупрозрачной конденсированной средой, обнаруживающее их существенное различие. В случае слоя из стекла им нельзя пренебречь, хотя в инфракрасной области оно значительно уменьшается в силу высокой поглощательной способности.